Check for updates

ChemistrySelect

Research Article
doi.org/10.1002/slct.202503764

Chemistry Europe
European Chemical Societies Publishing

www.chemistryselect.org

Green Synthesis, Characterization, and Multifunctional Bioactivity of *Thymus pectinatus*-Derived Silver Nanoparticles

Samed Şimşek*[a]

In this study, silver nanoparticles (AgNPs) were green-synthesized for the first time using the methanolic extract of *Thymus pectinatus* (TP), and their physicochemical properties as well as biological activities were systematically evaluated. The conversion and stabilization of Ag^{+} to Ag^{0} were confirmed by FTIR, XRD, and SEM-EDX analyses, which demonstrated the involvement of functional groups such as hydroxyl and amine. The synthesized TP-AgNPs exhibited high crystallinity with a dominant (111) XRD peak and spherical morphology (20–40 nm). Antioxidant analyses demonstrated that TP-AgNPs had superior activity compared to the extract, showing lower IC_{50} values in the DPPH$^{\bullet}$ (13.45 µg/mL) and $ABTS^{\bullet+}$ (5.67 µg/mL) assays, together with significantly higher reducing power (879.92 mg TE/g). Antifungal activity against *Monilinia fructigena* and *Verticillium dahliae* showed stronger inhibition (65.79% at 400 ppm), with lower LC_{50} values (298.96 and 267.34 ppm). In addition, TP-AgNPs demonstrated significantly stronger antibacterial activity, with wider inhibition zones and lower MICs compared to the extract. These findings confirm that TP-AgNPs exhibit multiple bioactivities, highlighting their potential as multifunctional agents.

1. Introduction

Natural products—particularly those of plant origin—have played a crucial role in pharmaceutical discovery and development. Their chemical diversity and wide range of bioactivities position them as promising candidates for drug development.[1] Due to their strong medicinal properties, plants have long been used in traditional medicine, contributing to the evolution of medical practices, and they exhibit diverse pharmacological effects, including antioxidant, anti-inflammatory, and antibacterial activities.[2,3] These properties contribute to the mitigation of oxidative stress, regulate inflammatory responses, and inhibit microbial growth, highlighting their therapeutic potential. In addition, their inherent molecular complexity often provides advantages over synthetic molecules by offering structurally diverse scaffolds that serve as valuable templates for drug design and optimization.[4]

In recent years, the exploration of botanical sources for pharmaceutical research has advanced considerably, contributing to the identification of numerous bioactive molecules, many of which have progressed to clinically approved drugs.[5] Developments in phytochemistry, metabolomics, and bioinformatics have further improved our ability to characterize, synthesize, and modify natural compounds, thus optimizing their pharmacokinetic and pharmacodynamic properties.[6,7] Additionally, innovative screening techniques and high-throughput methodologies have accelerated the discovery of novel bioactive molecules with significant therapeutic potential.

Within this context, the Lamiaceae family is considered one of the most important botanical groups, comprising 236 genera and an estimated 7133 species.[8] Among them, *Thymus* is one of the most common genera, with about 220 species.[9] Distributed across the Mediterranean, Asia, Europe, and North Africa, *Thymus* is widely recognized for its essential oil production and is among the most consumed medicinal plants worldwide. Traditionally, it has been used in the form of infusions and decoctions for oral hygiene, cough, digestive disorders, rheumatism, and menstrual complaints. In addition, several studies have demonstrated that *Thymus* species exhibit antibacterial, antioxidant, and antifungal properties.[8]

Beyond their traditional applications, *Thymus* species have attracted growing attention in contemporary medical research for their potential roles in disease prevention and therapy. Bioactive compounds from these plants are reported to contribute to the alleviation and prevention of conditions such as cardiovascular diseases, cancer, and neurodegenerative disorders.[10,11] Their cardioprotective effects may support vascular health, while their anticancer properties show promise in inhibiting tumor progression. Additionally, *Thymus* species are increasingly recognized for their neuroprotective effects, which may help prevent cognitive decline.[12,13] Given these benefits, *Thymus* species are considered valuable natural resources in both traditional and modern medicine, in addition to their commonly used culinary and aromatic uses.

Medicinal plants are widely recognized for their pharmacologically active compounds and their potential to control infections caused by both phytopathogens and human pathogens. Their dual role in agriculture and medicine renders them valuable resources in the development of sustainable antimicrobial strategies. In agriculture, pathogenic fungi such as *Monilinia fructigena* and *Verticillium dahliae* cause significant economic losses by infecting a wide range of crop species.[14,15] *M. fructi-*

[a] *Dr. S. Şimşek*
Department of Medical Services and Techniques, Çayırlı Vocational School, Erzincan Binali Yıldırım University, Erzincan 24500, Türkiye
E-mail: samed.simsek@erzincan.edu.tr

© 2025 Wiley-VCH GmbH

gena is responsible for fruit rot in apples, pears, plums, peaches, and cherries, while *V. dahliae* induces *Verticillium* wilt, characterized by leaf curling, vascular discoloration, and plant death.[16,17] Although fungicides are widely used in crop protection, fungal infections still cause significant global yield losses, estimated at 20% and 40% annually.[18] In addition, long-term reliance on chemical pesticides and antibiotics has raised serious concerns about environmental contamination, toxicological risks to humans and animals, and the spread of resistant microbial strains. In this context, biologically synthesized nanomaterials—especially plant-mediated silver nanoparticles—have attracted increasing interest due to their dual antimicrobial potential against both fungal and bacterial pathogens, offering eco-friendly solutions for agricultural and biomedical applications.

Nanotechnology has advanced significantly in the 21st century, resulting in the development and application of nanoparticles across various scientific disciplines.[19] Among these, nanoparticles with antimicrobial properties have become a major focus due to their potential applications in biomedical, pharmaceutical, and environmental areas.[20] Silver nanoparticles (AgNPs), in particular, have demonstrated significant antimicrobial activity, prompting the development of alternative synthesis approaches aimed at improving their performance and reducing associated environmental impacts.[21]

One of the most promising approaches in AgNP synthesis involves the use of plant-derived phytochemicals, commonly referred to as "green synthesis" This method employs plant extract-based reducing and stabilizing agents, providing an environmentally friendly alternative to traditional chemical methods, with advantages such as cost-effectiveness and biocompatibility.[22–24] AgNPs produced using this method have demonstrated potent antimicrobial activity against a variety of bacteria and fungi, suggesting their potential for treating microbial infections.[25,26] Additional benefits, including simplicity of production, low cost, high carrier capacity, and suitability for targeted drug delivery, further support their use in pharmaceutical applications.[27] Despite toxicity concerns, these advantages highlight their importance in nanotechnology. Green synthesis, based on biological processes and natural compounds, has gained attention for its sustainability and reduced environmental impact, in accordance with ecological standards in nanomaterial development.[27]

This study investigates the green synthesis and characterization of AgNPs using TP extract, with a focus on their antifungal, antibacterial, and antioxidant properties. To the best of our knowledge, this is the first reported application of TP in the eco-friendly synthesis of AgNPs with multiple bioactivities, highlighting their potential for biomedical use. Integrating phytotherapeutic knowledge with nanotechnology offers a sustainable strategy to combat phytopathogenic fungi, bacterial infections, and oxidative stress, while reducing reliance on synthetic fungicides, chemical antioxidants, and standard antibiotics. By harnessing the bioactive compounds in TP, this study proposes a cost-effective, nature-based alternative for crop disease management, antibacterial protection, and novel antioxidant strategies relevant to human health. It also highlights the interdisciplinary character of plant-mediated nanotechnology, which integrates botanical sciences, chemistry, and nanoscience in the development of significant synthesis methods. These findings provide a scientific basis for advancing green nanotechnology and expanding the applicability of AgNPs across diverse fields.

2. Results and Discussion

2.1. Fourier Transform Infrared (FTIR) Spectroscopy

FTIR spectroscopy was used to identify the functional groups involved in the synthesis and surface stabilization of AgNPs using the TP extract. Comparative spectral analysis of the extract and the TP-AgNPs demonstrated significant shifts and intensity changes in characteristic absorption bands, indicating the active participation of phytochemicals in the nanoparticle synthesis process (Figure 1).

FTIR spectrum confirmed the functional groups responsible for the reduction and stabilization of TP-AgNPs. The comparative analysis between the TP extract and TP-AgNPs demonstrated the formation of nanoparticles, as evidenced by characteristic shifts and altered band intensities. A broad absorption band around 3225 cm^{-1}, attributed to O—H and N—H stretching vibrations, reduced in intensity in the TP-AgNPs spectrum, suggesting the involvement of hydroxyl and amine groups in redox processes. The band at 2927 cm^{-1}, corresponding to aliphatic C—H stretching, also showed slight variations. A new peak at 3061 cm^{-1}, assigned to =C—H stretching of aromatic or alkenic structures, indicated the adsorption of phytochemicals on the nanoparticle surface. Signals at 1595 and 1515 cm^{-1}, corresponding to N—H deformation/amide I vibrations and aromatic C=C stretching, respectively, showed decreased intensity, pointing to the role of proteins and flavonoids in nanoparticle capping. Additional bands at 1397, 1258, 1160, and 1030 cm^{-1}, attributed to C—O stretching of alcohols, ethers, or phenolic groups, were shifted or reduced after synthesis, suggesting partial interaction of these groups during Ag^{+} reduction. Not all extract peaks disappeared after nanoparticle formation; only specific functional groups (e.g., hydroxyl, amine, aromatic C=C) were strongly involved, while in the synthesis, while others showed minimal changes or weak surface binding. These results indicate that phenolics, flavonoids, and proteins were the primary contributors to AgNP reduction and stabilization, consistent with previous reports highlighting the dual role of phytochemicals as both reducing and stabilizing agents.[28,29]

2.2. X-ray Diffraction (XRD)

X-ray diffraction (XRD) analysis confirmed the crystalline nature of the biosynthesized TP-AgNPs. Distinct peaks were observed at 2θ values of 38.1°, 44.1°, 64.3°, and 77.2°, corresponding to the (111), (200), (220), and (311) planes of face-centered cubic (fcc) silver crystals (JCPDS No. 04-0783). The most intense peak at 38.1° indicated preferred growth along the (111) plane, consistent with

© 2025 Wiley-VCH GmbH

23656549, 2025, 38, Downloaded from https://chemistry-europe.onlinelibrary.wiley.com/doi/10.1002/slct.202503764 by Samet MEK - Erzincan Universitesi , Wiley Online Library on [11/10/2025]. See the Terms and Conditions (https://onlinelibrary.wiley.com/terms-and-conditions) on Wiley Online Library for rules of use; OA articles are governed by the applicable Creative Commons License

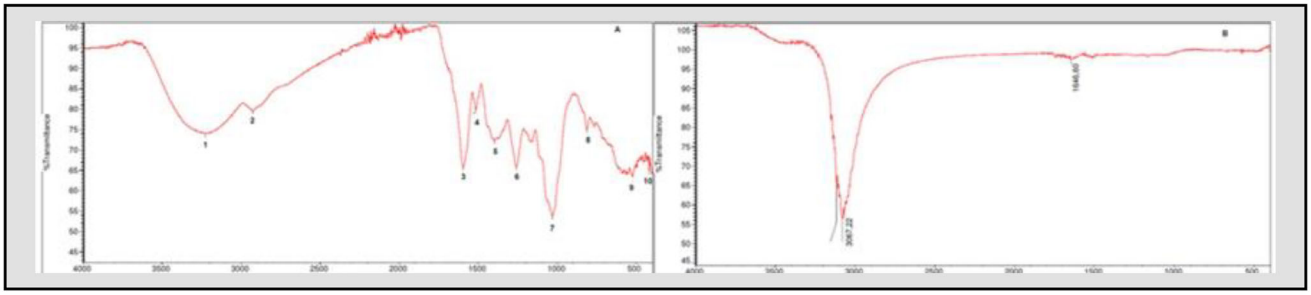


Figure 1. Fourier transform infrared spectra of the extract a) and AgNP b). 1: 3225, 2: 2927, 3: 1595, 4: 1515, 5: 1397, 6: 1258, 7: 1030, 8: 812, 9: 525, and 10: 418.

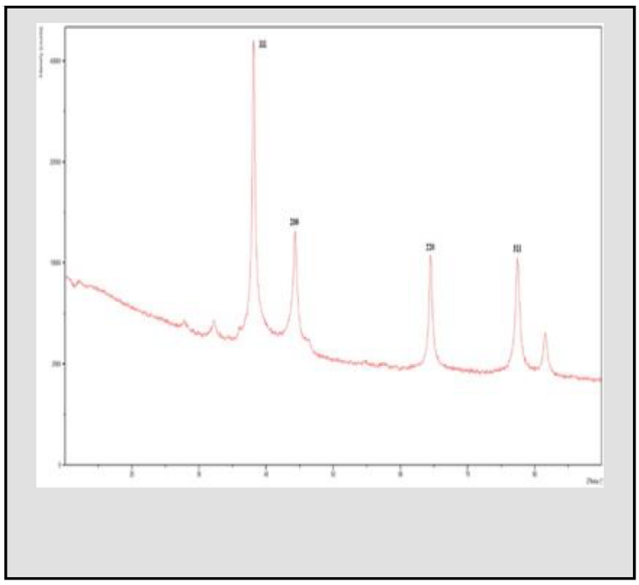


Figure 2. XRD pattern of TP-AgNPs.

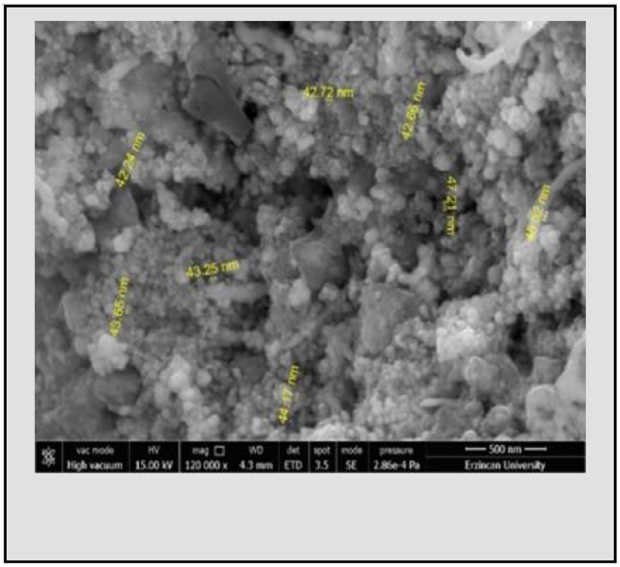


Figure 3a. Scanning electron microscopy images of the TP-AgNPs.

previous reports highlighting its thermodynamic stability during AgNP crystal formation (Figure 2).[30–32]

The sharp and well-defined diffraction peaks observed in the XRD pattern indicate a narrow crystallite size distribution, consistent with the nanocrystalline nature of the material. The average crystallite size (D) was calculated using the Debye–Scherrer equation:

$$D = K\lambda/\beta\cos\theta$$

where $K = 0.9$, $\lambda = 1.5406$ Å (Cu Kα), β is the full width at half maximum (FWHM) in radians, and θ is the Bragg angle. For the (111) plane at $2\theta = 38.1°$, with FWHM $= 0.4°$, the crystallite size was determined to be ~21 nm, confirming successful nanoparticle formation within the nanometer range.

In addition to silver peaks, minor diffraction peaks were detected at 2θ values near 29.9°, 32.3°, 36.2°, 46.4°, 65.3°, and 81.3°. These may be attributed to phytochemicals in the TP extract acting as capping and stabilizing agents or to the formation of trace amounts of silver oxide (Ag_2O) during synthesis. Such phytochemical constituents, typically of green synthesis protocols, contribute to colloidal stability and influence bio-interfacial interactions as a result of modifications of surface functional groups and zeta potential.[29,33,34] The predominance of the (111) diffraction peak suggests a preferential crystal orientation, which is often associated with increased surface energy and reactivity. This preferential orientation is particularly important for antimicrobial activity, as the high atomic density of the (111) plane facilitates interactions with microbial cell membranes and intracellular components.[35–37]

The high crystallinity of the TP-AgNPs is a key factor in determining their biological activity and catalytic performance. The absence of significant amorphous features suggests minimal interference from noncrystalline organic residues. These findings are consistent with previous reports indicating that green-synthesized AgNPs exhibit superior physicochemical characteristics relative to nanoparticles synthesized by conventional chemical methods.[38,39]

2.3. Scanning Electron Microscopy-Energy-Dispersive X-ray Spectroscopy (SEM-EDX) Analysis

The scanning electron microscopy (SEM) analysis revealed that the AgNPs synthesized using *Thymus* pectinatus methanol extract exhibited uniform spherical morphology with particle diameters between 20 nm and 40 nm. As shown in Figure 3a, the

© 2025 Wiley-VCH GmbH

23656549, 2025, 38, Downloaded from https://chemistry-europe.onlinelibrary.wiley.com/doi/10.1002/slct.202503764 by Samed MEK - Erzincan Universitesi , Wiley Online Library on [11/10/2025]. See the Terms and Conditions (https://onlinelibrary.wiley.com/terms-and-conditions) on Wiley Online Library for rules of use; OA articles are governed by the applicable Creative Commons License

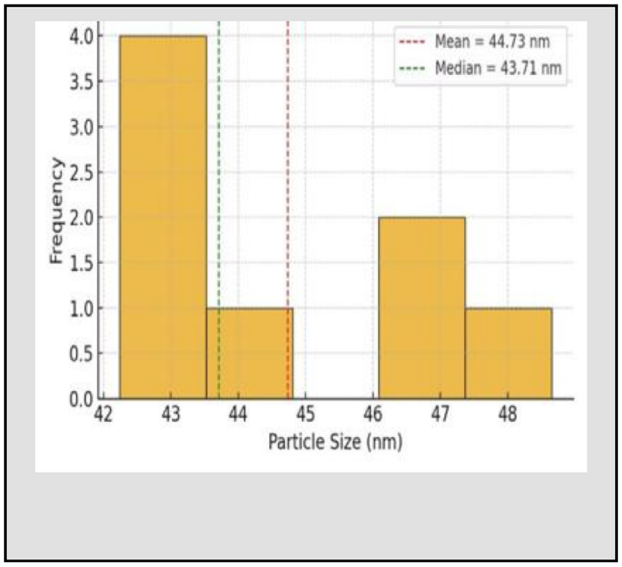


Figure 3b. Particle size distribution histogram of TP-AgNPs obtained from SEM images.

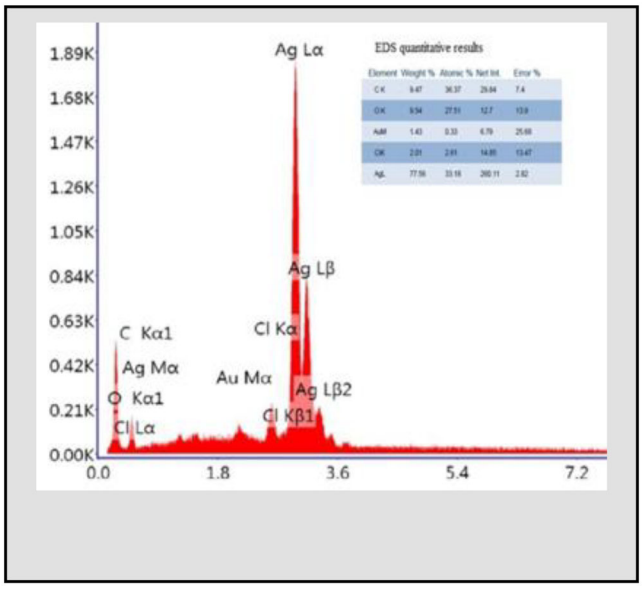


Figure 4. Energy dispersive X-ray spectrum and elemental analysis of TP-AgNPs.

particles exhibited well-defined surfaces, relatively uniform size distribution, and limited agglomeration. The spherical morphology represents a thermodynamically favored structure and is consistent with isotropic growth in the absence of strong facet-directing agents.[40,41] Particle size distribution analysis of 100 nanoparticles measured from SEM images revealed an average diameter of 44.7 ± 2.3 nm with a relatively uniform distribution (Figure 3b), confirming the morphological consistency observed in SEM micrographs.

Further confirmation of the nanoparticle composition was obtained using energy-dispersive X-ray (EDX) spectroscopy. As shown in Figure 4, a strong signal was observed at ~3 keV, corresponding to the characteristic surface plasmon resonance of elemental silver (Ag^0). Additional peaks for carbon and oxygen were also detected, attributed to the organic matrix of the TP extract that remains adsorbed on the nanoparticle surface. Such organic signatures are commonly observed in green-synthesised metallic nanoparticles due to the presence of plant-based capping layers.[42,43]

The morphological features (Figure 3a), together with the elemental analysis results (Figure 4), confirm the successful synthesis of TP-AgNPs. The controlled size, spherical shape, and surface uniformity of the nanoparticles produced by this green method are critical for potential applications in antimicrobial, antioxidant, and catalytic fields, where geometry and surface properties strongly influence their functional performance.

2.4. Antioxidant Assay

In this study, the antioxidant properties of TP methanolic extract and its TP-AgNP were systematically evaluated using various in vitro assays, including DPPH$^{\bullet}$ and ABTS$^{\bullet+}$, FRAP, TPC, and TFC. The AgNPs synthesized using TP demonstrated strong antioxidant activity, attributed to their bioactive compounds. The results, as shown in Table 1, demonstrate an increase in antioxidant capacity following TP-AgNP synthesis, suggesting that the phytochemical constituents are functionally active in the nanoparticle formulation.

The DPPH$^{\bullet}$ assay is one of the most widely used methods for evaluating the free radical scavenging capacity of plant-derived antioxidants, as it measures their ability to donate hydrogen atoms or electrons to neutralize free radicals. In this assay, the TP extract showed moderate activity with an IC_{50} of 25.83 ± 1.64 µg/mL, while TP-AgNPs exhibited significantly stronger activity (IC_{50}: 13.45 ± 1.88 µg/mL). Similarly, in the ABTS$^{\bullet+}$ assay, TP had an IC_{50} of 13.30 ± 1.75 µg/mL, compared to 5.67 ± 0.55 µg/mL for TP-AgNPs. These results indicate a twofold increase in antioxidant activity with nanoparticle formulation. The TP-AgNPs exhibited stronger radical scavenging activity not only compared to the extract but also relative to standard antioxidants such as ascorbic acid (8.25 ± 0.41 µg/mL), BHT (9.42 ± 0.63 µg/mL), BHA (6.33 ± 0.19 µg/mL), and Trolox (7.07 ± 0.15 µg/mL). Statistical analysis revealed that the IC_{50} values obtained from both the DPPH$^{\bullet}$ and ABTS$^{\bullet+}$ assays differed significantly among all samples ($p < 0.05$), indicating a significant increase in antioxidant capacity when the plant extract was used for the green synthesis of AgNPs.

When compared with other members of the genus, both the extract of TP and its nanoparticle form exhibited stronger activity than the hydroalcoholic extracts of *T. pubescens* (~31 µg/mL), *T. kotschyanus* (~47 µg/mL), and *T. daenensis* (~49 µg/mL),[44] relative to the highly active Anatolian species *T. cariensis* (DPPH IC_{50}: 34.97 µg/mL; ABTS IC_{50}: 9.98 µg/mL),[45] the extract showed higher potency in DPPH but lower in ABTS, while the nanoparticle form exhibited higher activity than *Thymus cariensis* in both tests, reflecting the influence of nanoparticle incorporation. Essential oils of some *Thymus* taxa, such as *Thymus capitatus* and *Thymus zygis*, displayed low antioxidant capacity, with high IC_{50} values (600–900 µg/mL for DPPH and 1410 µg/mL for

© 2025 Wiley-VCH GmbH

23656549, 2025, 38, Downloaded from https://chemistry-europe.onlinelibrary.wiley.com/doi/10.1002/slct.202503764 by Samed MEK - Erzincan Universitesi , Wiley Online Library on [11/10/2025]. See the Terms and Conditions (https://onlinelibrary.wiley.com/terms-and-conditions) on Wiley Online Library for rules of use; OA articles are governed by the applicable Creative Commons License

Table 1. Antioxidant activity of TP extract and AgNPs.

Example	DPPH$^{\bullet}$ scavenging IC_{50} (μg/mL)[a)]	$ABTS^{\bullet+}$ radical cation scavenging IC_{50} (μg/mL)[a)]	Reducing power mg TE $-g^{-1}$ extract[a)]	Total phenolics mg GAE g^{-1} extract[a)]	Total flavonoids mg QE g^{-1} extract[a)]
TP	25.83 ± 1.64^{c}	13.30 ± 1.75^{c}	49.79 ± 0.41^{a}	103.75 ± 0.71^{a}	34.95 ± 0.92^{a}
TP-AgNPs	13.45 ± 1.88^{b}	5.67 ± 0.55^{a}	879.92 ± 0.25^{e}	617.04 ± 0.56^{a}	142.86 ± 2.14^{a}
Trolox	8.50 ± 0.77^{a}	7.07 ± 0.15^{a,b}	–	–	–
BHA	8.04 ± 0.69^{a}	6.33 ± 0.19^{a,b}	338.57 ± 0.31^{c}	–	–
BHT	10.70 ± 0.73^{b}	9.42 ± 0.63^{b}	257.80 ± 1.24^{b}	–	–
Ascorbic acid	9.91 ± 0.87^{a,b}	8.25 ± 0.4^{a,b}	394.17 ± 0.98^{d}	–	–

[a)] Values are expressed as mean ± standard deviation ($n = 3$).
[a–e]Different letters in the same column indicate statistical difference ($p < 0.05$).

ABTS),[46] and even the relatively active oil of *Thymus sipyleus* (IC_{50} ~220 μg/mL for DPPH) showed lower activity than both the extract and its AgNPs.[47] *Thymus vulgaris* polar extracts show IC_{50}/EC_{50} values of 1.8–44.7 μg/mL in the DPPH assay, while its phenolic-rich fractions exhibit stronger activity with ABTS values of 0.7–13.8 μg/mL,[48] in this context, TP is within the range of polar extracts, and the nanoparticle formulation approaches the activity of the phenolic-rich fractions. Beyond extracts and essential oils, several reports have investigated AgNP formulations of different *Thymus* species. *Thymus serpyllum*-AgNPs exhibited potent DPPH scavenging activity with an IC_{50} of ~10 μg/mL,[49] comparable to the present material, while *T. vulgaris*-AgNPs have shown highly variable results, from very strong DPPH activity (~97% inhibition at 1000 μg/mL)[50] to relatively low activity with an IC_{50} of ~794 μg/mL,[51] indicating that synthesis parameters and phytochemical composition are important determinants of antioxidant capacity. Overall, the nanoparticles obtained in the present study, with IC_{50} values of 13.45 μg/mL (DPPH) and 5.67 μg/mL (ABTS), can be considered among the most active *Thymus*-derived AgNPs reported to date, indicating an increase in antioxidant capacity with nanoparticle incorporation.

The comparative analysis of reducing power between TP and TP-AgNP shows a significant increase in antioxidant potential, which may be attributed to the integration of nanoparticles. While TP extract exhibited a reducing capacity of 49.79 ± 0.41 mg TE/g extract, TP-AgNP showed a significantly higher value of 879.92 ± 0.25 mg TE/g extract—an 18-fold increase. This observed increase indicates that the high surface-area-to-volume ratio of AgNPs supports electron transfer and stabilizes phytocompounds by surface interactions, which increases the electron-donating ability of the phytoconstituents. In addition, TP-AgNP demonstrated superior reducing capacity compared to standard antioxidants such as BHA (338.57 ± 0.31), BHT (257.80 ± 1.24), and ascorbic acid (394.17 ± 0.98 mg TE/g extract). Statistical analysis confirmed that the values differed significantly among all tested samples ($p < 0.05$). In relation to other *Thymus* species, the reducing capacity of TP extract is comparable to that of *T. vulgaris* leaf extracts from Saudi Arabia, where FRAP values of about 58 mg TE/g DW were reported under optimized extraction conditions,[52] and to *T. vulgaris* extracts obtained by Soxhlet extraction (~74 mg TE/g dry extract).[53] However, TP-AgNPs showed values (~880 mg TE/g) far higher than those reported. Even ultrasound-assisted extraction of thyme, which showed values around 527 mg TE/g DW,[54] was still lower than TP-AgNPs, and methanolic extracts of *Thymus mastichina* also showed variation among samples, but none were as strong.[55] Essential oils of *Thymus* species such as *T. vulgaris* and *Thymus spicata* exhibited low ferric reducing power, with values in the low μM Fe^{2+}/g range,[56] while reports on *Thymus algeriensis* and *T. capitatus* reported only moderate antioxidant activity; in comparison, both the TP extract and its AgNPs demonstrated significantly stronger activity.[57] These comparisons show that although TP extract exhibits activity similar to other active members of the genus, its nanoparticle formulation results in a higher reducing power than previously reported, highlighting its novelty and potential applications.

The significantly higher antioxidant activity of TP-AgNP was supported by phytochemical analyses, particularly the elevated total phenolic and flavonoid contents. The TPC of TP-AgNP was determined as 617.04 ± 0.56 mg GAE/g extract compared with 103.75 ± 0.71 mg GAE/g in TP, indicating a sixfold increase. Similarly, TFC increased from 34.95 ± 0.92 mg QE/g in TP to 142.86 ± 2.14 mg QE/g in TP-AgNP, and both parameters differed significantly ($p < 0.05$). Elevations in both TPC and TFC have also been reported for AgNPs synthesized from various plant extracts, where nanoparticle formation enhanced phenolic content and overall antioxidant capacity, in line with previous reports.[58,59] Compared with other *Thymus* species, these values are significant. For *T. vulgaris* extracts, typically show TPC/TFC levels of 15–32 mg GAE/g and 6–8 mg QE/g, while studies across 14 taxa report ~31–71 mg GAE/g and 1.9–8.1 mg QE/g, all lower than TP-AgNP and, in many cases, even the TP extract.[60] Regional studies on *T. serpyllum* and related taxa reported 20–90 mg GAE/g DW,[61] and Tunisian species such as *T. algeriensis* (~19 mg GAE/g DW) and *Thymus herba-barona* (~236 mg GAE/g extract; ~47 mg/g dry plant) also were lower than the nanoparticle values, with the latter comparable only to TP extract.[62] Even higher reports, such as ~108–122 mg GAE/g dry plant in

© 2025 Wiley-VCH GmbH

23656549, 2025, 38, Downloaded from https://chemistry-europe.onlinelibrary.wiley.com/doi/10.1002/slct.202503764 by Samed MEK - Erzincan Universitesi , Wiley Online Library on [11/10/2025]. See the Terms and Conditions (https://onlinelibrary.wiley.com/terms-and-conditions) on Wiley Online Library for rules of use; OA articles are governed by the applicable Creative Commons License

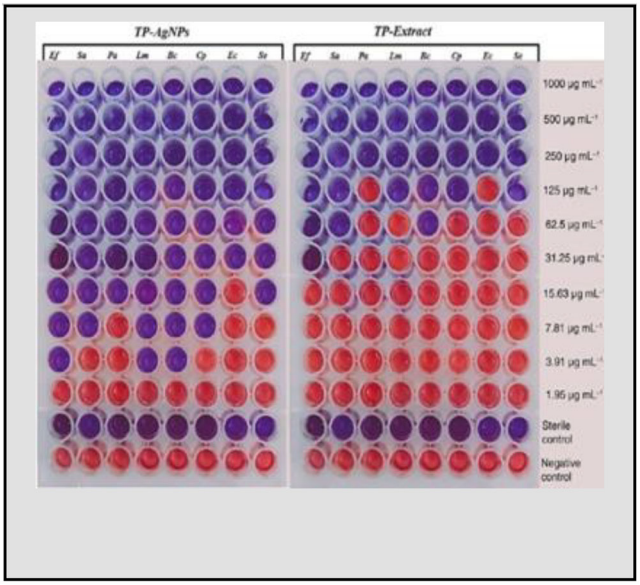


Figure 5. Minimum inhibitory concentration analysis of TP- extract and TP-AgNPs. Ef: *E. faecium*, Sa: *S. aureus*, Pa: *P. aeruginosa*, Lm: *L. monocytogenes*, Bc: *B. cereus*, Cp: *C. perfringens*, Ec: *E. coli*, Se: *S. enteritidis*.

polyphenolic extracts or ultrasound-optimized extractions, did not exceed the value observed for TP-AgNP.[63] Aqueous decoctions of species such as *T. zygis*, *Thymus pulegioides*, and *Thymus caespititius* showed ~79–391 mg GAE/g,[64] approaching the values of TP-AgNP, although without the increase observed in this study. These findings demonstrate that nanoparticle formulation not only improves the phytochemical profile of TP but also results in values higher than most reported for the genus, highlighting its potential as a potent natural antioxidant source for nutraceutical and therapeutic applications.

2.5. Antibacterial Activity

In the present study, the antimicrobial properties of TP and TP-AgNPs were comprehensively evaluated against a panel of clinically relevant Gram-positive and Gram-negative bacterial strains. Antimicrobial properties were assessed using disc diffusion and MIC assays, and the results demonstrated that the presence of silver nanoparticles significantly improved the antimicrobial activity of the plant extract. The findings are presented in Figure 5 and Table 2.

The disc diffusion assay results indicated that TP-AgNPs produced larger inhibition zone diameters compared to TP extract alone across all tested bacterial strains. The inhibition zone diameter against *Staphylococcus aureus* increased from 10.2 ± 0.5 mm with TP extract to 35.5 ± 1.2 mm for TP–AgNPs, according to the agar disc diffusion assay. Similar increases in inhibition zones were observed for *Enterococcus faecium*, *Escherichia coli*, and *Salmonella enteritidis*, with diameters increasing from 6.6, 9.3, and 7.0 mm to 28.0, 28.8, and 30.4 mm, respectively. *Pseudomonas aeruginosa*, known for its high intrinsic resistance, showed an increase in inhibition zone diameter from 5.2 ± 0.8 mm with TP to 22.3 ± 2.0 mm with TP-AgNPs, and in several strains, the inhibition zones obtained with TP-AgNPs were comparable to or larger than those produced by imipenem. Statistical analysis revealed that the inhibition zone diameters differed significantly among treatments for each bacterium ($p < 0.05$), indicating that the antibacterial activities of TP, TP-AgNPs, and imipenem were statistically distinct.

The MIC results were consistent with the disc diffusion findings, indicating a stronger antimicrobial effect for TP-AgNPs compared to TP extract. The MIC value for *Listeria monocytogenes* was reduced from 125 µg/mL with TP extract to 3.91 µg/mL with TP-AgNPs, indicating over a 30-fold increase in antibacterial potency. MIC values were also found to be lower in other tested strains, including *E. faecium*, *Bacillus cereus*, and *Clostridium perfringens*, when treated with TP-AgNPs, and in some cases were similar to or lower than those recorded for tetracycline. These findings are consistent with previous studies that demonstrated higher antibacterial activity of silver nanoparticles synthesized using plant extracts compared to the individual components alone.[65,66]

When compared with other *Thymus* species, our findings reveal both parallels and distinctive differences. Vardar-Ünlü et al. (2003) reported that TP essential oil, rich in thymol, carvacrol, γ-terpinene, and *p*-cymene, exhibited strong antimicrobial activity, while the methanolic extract showed only limited to moderate effects.[67] These findings are in agreement with the present study, where the TP extract produced restricted inhibition zones and elevated MIC values. Similarly, Akman et al. (2024) observed MIC values of 31.25 µg/mL for TP extract against *S. aureus*,[1] consistent with the limited activity recorded here, while TP-AgNPs achieved significantly lower MICs, highlighting the contribution of nanoparticle formulation. Similar patterns have been documented in other *Thymus* species, where essential oils generally show higher antimicrobial potency compared to extracts. *T. daenensis* oil showed inhibition zones of 39 mm against *S. aureus*, at times higher than those of standard antibiotics,[68] and *T. capitatus* oil, dominated by carvacrol and thymol, was strongly active against both *Staphylococcus* and *Enterobacteriaceae*.[69] Consistent with these reports, TP-AgNPs demonstrated strong inhibition against *S. aureus*, in contrast to the lower activity of TP extract. Similarly, *T. serpyllum* essential oil inhibited *P. aeruginosa* with a 17 mm zone and an MIC of ~134 µg/mL,[70] values lower than the 22 mm zone and 3.91–15.6 µg/mL MICs obtained for TP-AgNPs, indicating that nanoparticle formulation resulted in activities comparable to or higher than those of active *Thymus* oils. Additional evidence from *T. vulgaris* supports these observations, as its essential oil has been reported to show strong effects against *S. aureus*, *E. coli*, and carbapenem-resistant *Acinetobacter baumannii*, with inhibition zones ≥ 20 mm and MIC values as low as 0.3–1.25 mg/mL.[71] While the TP extract exhibited lower activity, TP-AgNPs demonstrated inhibition zones and MICs similar to or higher than those of *T. vulgaris* oils. Similarly, *T. pannonicus* essential oil demonstrated activity against *S. aureus* and *E. coli* but only limited effects on *P. aeruginosa* (MIC ~ 200 µL/mL),[72] in contrast to the pronounced inhibition observed with TP-AgNPs against this resistant pathogen.

© 2025 Wiley-VCH GmbH

23656549, 2025, 38, Downloaded from https://chemistry-europe.onlinelibrary.wiley.com/doi/10.1002/slct.202503764 by Samed MEK - Erzincan Universitesi , Wiley Online Library on [11/10/2025]. See the Terms and Conditions (https://onlinelibrary.wiley.com/terms-and-conditions) on Wiley Online Library for rules of use; OA articles are governed by the applicable Creative Commons License

23656549, 2025, 38, Downloaded from https://chemistry-europe.onlinelibrary.wiley.com/doi/10.1002/slct.202503764 by Samed MEK - Erzincan Universitesi , Wiley Online Library on [11/10/2025]. See the Terms and Conditions (https://onlinelibrary.wiley.com/terms-and-conditions) on Wiley Online Library for rules of use; OA articles are governed by the applicable Creative Commons License

Table 2. Antibacterial activities of TP and TP-AgNPs.

Bacterias	Disc diffusion (mm)[a)]			MIC (μg/mL)		
	TP	TP-AgNPs	Imipenem[a)]	P	TP-AgNPs	Tetracycline[a)]
E. faecium	6.6 ± 0.4^{c}	28.0 ± 1.5^{b}	45.0 ± 1.0^{a}	31.25	3.91	1.95
S. aureus	10.2 ± 0.5^{c}	35.5 ± 1.2^{b}	45.3 ± 0.6^{a}	62.5	7.81	7.81
P. auroginosa	5.2 ± 0.8^{b}	22.3 ± 2.0^{a}	24.3 ± 2.5^{a}	250	15.62	3.91
L. monocytogenes	9.5 ± 0.3^{c}	26.0 ± 1.8^{b}	36.3 ± 2.1^{a}	125	3.91	3.91
B. cereus	11.1 ± 0.6^{c}	23.5 ± 1.4^{b}	30.0 ± 1.0^{a}	62.5	3.91	7.81
C. perfringens	8.7 ± 0.5^{c}	21.1 ± 1.3^{a}	17.0 ± 1.0^{b}	125	7.81	1.95
E. coli	9.3 ± 0.2^{c}	28.8 ± 2.0^{b}	35.3 ± 2.1^{a}	250	31.25	7.81
S. enteriditis	7.0 ± 0.4^{c}	30.4 ± 1.6^{b}	43.3 ± 1.5^{a}	125	15.62	3.91

[a)] Positive control (imipenem and tetracycline), inhibition zone diameters in mm (mean ± sd, $n = 3$).
[a–c]Different letters in the same row indicate statistical difference ($p < 0.05$).

Green-synthesized silver nanoparticles from other *Thymus* species have shown results consistent with our observations. *T. kotschyanus* AgNPs exhibited strong activity against Gram-positive strains such as *S. aureus* and *B. cereus*,[73] while *T. serpyllum* AgNPs also showed greater antibacterial effects compared with extracts, particularly against Gram-positive bacteria.[74] Similarly, *T. vulgaris*-derived AgNPs demonstrated both antimicrobial and antioxidant properties,[75] and more recent studies reported MIC values of ~31.5 μg/mL against multidrug-resistant *E. faecalis*.[76] In contrast, TP-AgNPs in the present study demonstrated MIC values as low as 3.91 μg/mL against *L. monocytogenes*, indicating higher potency. They were effective not only against Gram-positive bacteria but also against Gram-negative species such as *E. coli* and *P. aeruginosa*, which are typically more resistant due to their outer membrane barrier. Overall, while the TP extract exhibited antimicrobial activity comparable to nonvolatile *Thymus* extracts reported previously, nanoparticle formulation significantly improved its activity. TP-AgNPs produced inhibition zones and MIC values on par with or higher than those of essential oils from several *Thymus* species. Importantly, their pronounced activity against resistant Gram-negative bacteria indicates their potential as a broad antimicrobial system, with specific advantages over previously reported *Thymus*-based AgNP formulations

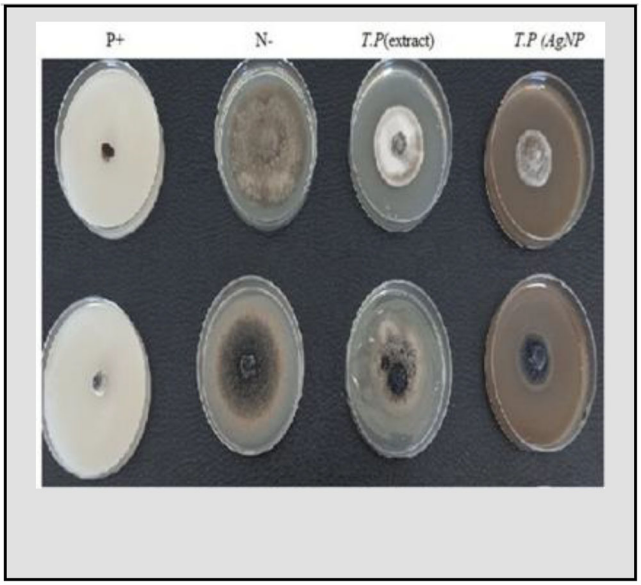


Figure 6. Antifungal activity of TP extract and AgNPs. T.P: *T. pectinatus*, M.F: *M. fructigena*, V.D: *V. dahliae*, N−: negative control, P+: positive control (Thiram. 80%).

Table 3. Antifungal activity of TP extract and AgNPs.

Doses (ppm)	TP[a)]		TP-AgNPs[a)]	
	M.F	V.D	M.F	V.D
P+	100 ± 0.00^{a}	100 ± 0.00^{a}	100 ± 0.00^{a}	100 ± 0.00^{a}
50	3.92 ± 2.81^{e}	0.00 ± 0.0^{e}	2.06 ± 2.06^{e}	3.99 ± 2.87^{e}
100	15.68 ± 1.47^{d}	10.16 ± 1.43^{d}	12.95 ± 5.11^{d}	21.71 ± 4.12^{d}
200	30.55 ± 1.47^{c}	28.89 ± 0.75^{c}	32.73 ± 1.86^{c}	35.04 ± 1.16^{c}
400	51.83 ± 0.44^{b}	49.99 ± 0.43^{b}	61.92 ± 3.30^{b}	65.79 ± 0.69^{b}
N−	0.00 ± 0.0^{f}	0.00 ± 0.0^{e}	0.00 ± 0.0^{e}	0.00 ± 0.0^{e}

[a)] [a-e]Different letters in the same row indicate statistical difference ($p < 0.05$), T.P; *T. pectinatus*, M.F; *M. fructigena*, V.D; *V. dahliae*, N−; negative control (DMSO), P+; positive control (Thiram 80%).

2.6. Antifungal Activity

The antifungal activity of TP extract and its synthesized TP-AgNPs was evaluated against the phytopathogens *M. fructigena* and *V. dahliae* at different concentrations (50–400 ppm) using the agar diffusion method (Figure 6). The observed inhibition rates are shown in Table 3, while the lethal concentration (LC_{50}) values are shown in Table 4.

Evaluation of antifungal activity showed that both the methanol extract of TP and its TP-AgNPs exhibited concentration-dependent inhibitory effects against *M. fructigena* and *V. dahliae*. TP-AgNPs showed significantly higher activity than the extract at 400 ppm, with inhibition values of 61.92% against *M. fructigena* and 65.79% against *V. dahliae*, indicating

© 2025 Wiley-VCH GmbH

Table 4. Lethal dose values (ppm) of TP plant extract and AgNP against test microorganisms.

Plant	LC values	Test microorganisms[a]	
		M.F	V.D
TP	LC_{50} (ppm)	367.38	371.43
	Slope	1.89 ± 0.41	2.47 ± 0.0.29
	Chi-square	0.513	3.21
TP-AgNPs	LC_{50} (ppm)	298.96	267.34
	Slope	2.49 ± 0.266	2.19 ± 0.24
	Chi-square	0.310	2.64

[a] LC: Effective dose (letal consantrion), Low. = lower bound (95% limits), Upr. = upper bound (95% limits), Het. = heterogeneity, X^2 = Chi-square (goodness of fit, $p > 0.05$), M.F: *Monilinia fructigena*, V.D: *Verticillium dahlia*.

strong antimicrobial effects. In contrast, the TP extract showed lower inhibition values of 51.83% and 49.99%, respectively. These findings suggest that while the extract has antifungal activity, this activity increases when formulated as AgNPs.

The increased antifungal activity of TP-AgNPs was further supported by LC_{50} analysis, which showed significantly lower LC_{50} values compared to the methanol extract. TP-AgNPs exhibited LC_{50} values of 298.96 ppm against *M. fructigena* and 267.34 ppm against *V. dahliae*, while the extract showed higher values of 367.38 and 371.43 ppm, respectively. For comparison, the positive control (Thiram 80%) exhibited complete inhibition (100%) against both fungal strains, and statistical analysis ($p < 0.05$) confirmed that TP-AgNPs had significantly higher antifungal activity than the extract, although lower than the fungicide standard. Additionally, probit regression analysis provided quantitative data, with higher slope values for TP-AgNPs indicating stronger dose-dependent antifungal effects. A higher slope value was observed for *M. fructigena* (2.49 ± 0.266), indicating a stronger dose-dependent antifungal effect.

When compared with other *Thymus* species, the antifungal activity of the TP extract can be considered moderate, while TP-AgNPs approach the levels typically reported for thymol/carvacrol-rich oils and advanced nanoformulations. *T. vulgaris* essential oil strongly inhibits *Candida albicans*, *C. glabrata*, and *A. fumigatus*, attributed to its high thymol and carvacrol content,[77,78] and *T. daenensis* oil encapsulated in chitosan nanoparticles exhibited potent effects against *C. parapsilosis* (MIC 0.032–1 µg/mL) while inhibiting the virulence gene BCR1.[79] Similarly, *T. albicans* and *T. broussonetii* show strong antifungal activity against dermatophytes, *C. neoformans*, and *Candida* spp., attributed to constituents such as 1,8-cineole, linalool, and α-terpineol.[80,81] In contrast, species such as *T. fallax* and *T. serpyllum* generally exhibit lower antifungal activity or higher MICs, especially in crude extracts.[82,83] In this context, TP extract is consistent with the moderate activity of *T. serpyllum* and *T. fallax*, while TP-AgNPs exhibit significantly higher potency, with inhibition values comparable to the most active oils of *T. vulgaris* and *T. daenensis*. These findings are consistent with previous reports showing that nanoemulsions or nanoparticle formulations of *Thymus* oils—such as *T. vulgaris* nanoemulsions[84] or carvacrol-loaded chitosan nanoparticles[85]—demonstrate higher antifungal activity than crude extracts.

The superior antifungal activity of TP-AgNPs compared to the extract can be attributed to the characteristic physicochemical properties of silver nanoparticles. Their high surface area-to-volume ratio and nanoscale size increase interactions with fungal cell walls and membranes, resulting in structural changes such as membrane disruption, vacuolization, and cytoplasmic leakage.[86,87] The lower LC_{50} values and higher regression slopes observed for TP-AgNPs quantitatively support their stronger antifungal activity, which may be attributed to the optimized physicochemical properties of the silver matrix. The strong inhibition of *V. dahliae*, a highly resistant phytopathogen, is of particular interest. These findings highlight the potential of plant-mediated nanoparticle formulations as promising antifungal agents, demonstrating stronger activity than crude extracts.

3. Conclusion

This study demonstrated, for the first time, the successful green synthesis of silver nanoparticles using TP methanolic extract. Structural analyses, including FTIR, XRD, SEM, and EDX, confirmed the formation of crystalline and stable TP-AgNPs. Phytochemicals, particularly phenolics and flavonoids, contributed to nanoparticle stabilization and to the observed antioxidant and antimicrobial activities. The high crystallinity and absence of significant amorphous features further supported the purity and stability of the synthesized nanostructures. Biological evaluations demonstrated that TP-AgNPs exhibited significantly higher bioactivities compared to the extract. Antioxidant tests (DPPH$^{\bullet}$ and ABTS$^{\bullet+}$) showed stronger radical scavenging potential, which may be attributed to the synergistic action of phenolic compounds and the silver core. In antimicrobial assays, TP-AgNPs demonstrated significant antibacterial activity against both Gram-positive and Gram-negative strains, as well as strong antifungal effects against phytopathogens such as *V. dahliae* and M. *fructigena*. These findings highlight the importance of nanoparticle morphology and surface chemistry in determining biological activity. Overall, the results highlight TP as a novel and valuable source for the eco-friendly production of bioactive silver nanoparticles. The superior antioxidant and antimicrobial properties of TP-AgNPs suggest potential applications not only in pharmaceutical and biomedical contexts but also in agriculture as a natural alternative to synthetic pesticides and fungicides. Future studies focusing on in vivo assessments and mechanistic evaluations will further clarify their practical applicability and safety.

4. Experimental Section

4.1. Chemicals and Instrumentation

All chemicals and solvents of analytical grade used in this study were purchased from Sigma-Aldrich. Fourier 'transform infrared

© 2025 Wiley-VCH GmbH

23656549, 2025, 38, Downloaded from https://chemistry-europe.onlinelibrary.wiley.com/doi/10.1002/slct.202503764 by Samed MEK - Erzincan Universitesi , Wiley Online Library on [11/10/2025]. See the Terms and Conditions (https://onlinelibrary.wiley.com/terms-and-conditions) on Wiley Online Library for rules of use; OA articles are governed by the applicable Creative Commons License

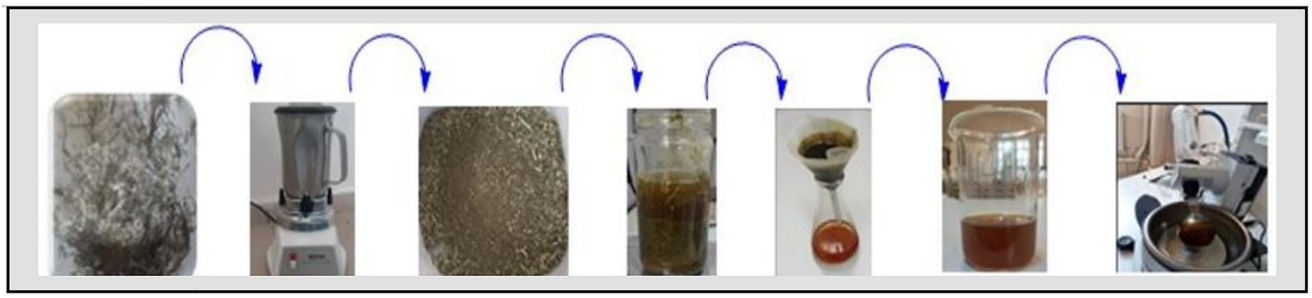


Figure 7. Extract from the aerial parts of *T. pectinatus*.

(FTIR) measurements were performed using a Jasco FTIR 4700 spectrometer, and scanning electron microscopy (SEM) analysis was conducted using a Quanta FEG450.

4.2. Plant Materials

The TP was collected from Erzincan province during the inflorescence period. The plant sample was authenticated by Prof. Dr. Ali Kandemir (Erzincan Binali Yıldırım University, Faculty of Art and Sciences, Department of Biology). Authentic samples (ID number of TP: 6735) were deposited in the herbarium of Erzincan Binali Yıldırım University (EBYU). The aerial parts of plant material were dried at room temperature and in the shade for the extraction process.

4.3. Extraction

The air-dried aerial parts of TP were well-grounded using a lab mill. Solid–liquid extraction was applied to the powdered plant material (500 g).[88] Maceration was conducted with methanol (3 × 500 mL, 3 × 12 h). After each extraction, the same plant residue was re-extracted with fresh methanol, and the filtrates were combined. The resulting extracts were concentrated under vacuum at 40 °C and 100 rpm using a rotary evaporator. The extract obtained was stored in dark flasks at +4 °C until AgNPs with antifungal activity were prepared (Figure 7).

4.4. AgNP Synthesis

The methanol extract of TP (3.0 g) was dissolved in pure water (900 mL). The silver nitrate solution (0.024 M, 900 mL) was slowly added to the extract solution. The final reaction mixture was stirred at 55 °C for 3 h. The color change from yellowish-brown to dark brown/black indicated the formation of TP-AgNPs. The mixture was cooled to room temperature, centrifuged at 15,000 rpm for 15 min, and washed with distilled water. After drying by lyophilization, TP-AgNPs were obtained (Figure 8).

4.5. Identification of Nanoparticles

The nanoparticle structure was clarified using comprehensive spectrophotometric studies. Fourier transform infrared (FTIR) spectroscopy provided information about functional group changes during biological reduction as a result of the study. The X-ray diffraction (XRD) pattern was recorded with an Empyrean Malvern Panalytical diffractometer using Cu Ka radiation. Scanning electron microscopy (SEM) analysis (Quanta FEG450) was performed to determine the nanoparticle properties.

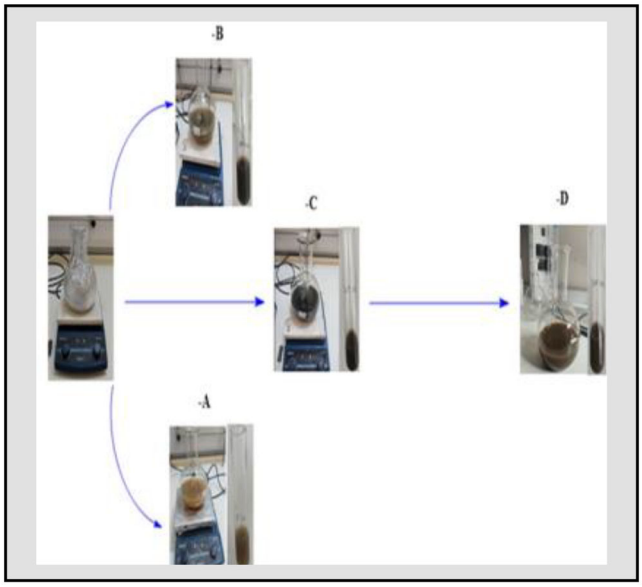


Figure 8. Time-dependent color change observed during the biosynthesis of AgNPs using *T. pectinatus* aerial parts extract. a) 5 min, b) 10 min, c) 20 min, and d) 30 min. The gradual transition from brown to dark brown/black indicates the formation of silver nanoparticles.

4.6. DPPH Radical Scavenging Capacity

The free radical-scavenging activity of the extract and AgNPs was evaluated using a previously described DPPH• method.[89,90] A 0.26 mM DPPH• (2,2-diphenyl-1-picrylhydrazyl) methanolic solution was prepared, and 1 mL of this solution was mixed with 3 mL of the sample solution (1–1000 µL). After vortexing, the mixture was incubated at room temperature in the dark for 30 min. All tests were performed in triplicate ($n = 3$). Absorbance was measured at 517 nm. DPPH• activity was calculated as:

$$\text{Activity}\ (\%) = [(A_0 - A_1)\,/A_0] \times 100$$

where A_0 is the control absorbance and A_1 is the sample absorbance. All experiments were performed in triplicate, and results are expressed as mean ± standard deviation in µg/mL (IC_{50}).

4.7. Ferric Reducing Power (FRAP)

The reducing power of the extract and AgNPs was evaluated using previously reported modified methods.[91,92] Briefly, 1.0 mL of phosphate buffer (0.2 M, pH 6.6) and 1.25 mL of $[K_3Fe(CN)_6]$ were mixed with 250 µL of the sample and incubated at 50 °C

© 2025 Wiley-VCH GmbH

23656549, 2025, 38, Downloaded from https://chemistry-europe.onlinelibrary.wiley.com/doi/10.1002/slct.202503764 by Samed MEK - Erzincan Universitesi , Wiley Online Library on [11/10/2025]. See the Terms and Conditions (https://onlinelibrary.wiley.com/terms-and-conditions) on Wiley Online Library for rules of use; OA articles are governed by the applicable Creative Commons License

23656549, 2025, 38, Downloaded from https://chemistry-europe.onlinelibrary.wiley.com/doi/10.1002/slct.202503764 by Samed MEK - Erzincan Universitesi , Wiley Online Library on [11/10/2025]. See the Terms and Conditions (https://onlinelibrary.wiley.com/terms-and-conditions) on Wiley Online Library for rules of use; OA articles are governed by the applicable Creative Commons License

for 20 min. After incubation, 1.25 mL of 10% TCA and 0.25 mL of 0.1% $FeCl_3$ were added. Absorbance was measured at 700 nm. All tests were performed in triplicate ($n = 3$). Results were expressed as mg Trolox equivalent (TE)/g extract using a calibration curve (10–100 µg/mL Trolox). BHT, BHA, and ascorbic acid were used as standard antioxidants for comparison.

4.8. $ABTS^{\bullet+}$ Assay

The cationic radical-scavenging activities of the extract and AgNPs were evaluated using a modified method described by Şimşek et al. and Albayrak et al.[93,94] A 2 mM ABTS and 2.45 mM $K_2S_2O_8$ solution was prepared in 0.1 M phosphate buffer (pH 7.4), mixed in a 1:2 ratio, and incubated in the dark for 12 h to generate $ABTS^{\bullet+}$. Test samples and standards (1 mg/mL) were prepared, and different volumes (1–1000 µL) were diluted to 3 mL with phosphate buffer. Then, 1 mL of $ABTS^{\bullet+}$ solution was added, vortexed, and incubated at room temperature for 60 min. All tests were performed in triplicate ($n = 3$). Absorbance was measured at 734 nm, and radical scavenging activity was calculated as percent inhibition. IC_{50} values (µg/mL) were determined and compared with Trolox, BHA, BHT, and ascorbic acid.

4.9. Total Phenolic Content (TPC)

The TPC of the extracts was determined spectrophotometrically using the Folin–Ciocalteu method.[95,96] Briefly, 100 µL of extract or standard solution (1 mg/mL) was mixed with 4.5 mL distilled water and 100 µL of Folin–Ciocalteu reagent, followed by incubation at room temperature for 120 min. Then, 300 µL of 2% Na_2CO_3 was added, and the mixtures were vortexed. Absorbance was measured at 760 nm. All tests were performed in triplicate. A calibration curve ($y = 0.117x - 0.011$) was generated using gallic acid (1–1000 µg/mL), and results were expressed as mg gallic acid equivalent per gram extract.

4.10. Total Flavonoid Content (TFC)

The total flavonoid content (TFC) of the extracts was assessed following the procedure of Gözcü et al.[97,98] 100 µL of extract and standard solutions (1 mg/mL) were mixed with 4.7 mL of methanol. Then, 100 µL of NH_4CH_3COO (1 M) and 100 µL of $AlCl_3$ (10%) were added. The mixtures were vortexed and incubated at room temperature for 45 min. Absorbance was measured at 415 nm. All tests were performed in triplicate. Results were expressed as mg quercetin equivalent per gram extract using a calibration curve ($y = 0.117x - 0.011$) generated from quercetin concentrations (1–1000 µg/mL).

4.11. Antibacterial Activity

Disc diffusion method[99] and minimum inhibitory concentration (MIC) assays[100] were used to determine the antibacterial activity of the TP and TP-AgNPs. The study involved eight bacterial strains: five Gram-positive (*L. monocytogenes* (ATCC 51,774), *S. aureus* (ATCC 6538), *B. cereus* (ATCC 10,876), *C. perfringens* (ATCC 13,124), and *E. faecium* (ATCC 8459)) and three Gram-negative (*P. aeruginosa* (ATCC 15,442), *E. coli* (ATCC 25,922), and *S. enteritidis* (ATCC 13,076)) For the disc diffusion assay, PCA plates were inoculated with 100 µL of each bacterial suspension at a concentration of 10^8 cfu/mL. Sterile discs were loaded with 5 µL of the samples dissolved in 10% DMSO. As a positive control, an imipenem disc was included. After 24-h incubation at 37 °C, inhibition zones were measured using a digital caliper.

A resazurin-based 96-well microdilution assay with slight modifications was performed to determine the MIC values. Sterile nutrient broth (50 µL) was dispensed into wells of rows 2–10. In the first row, 100 µL of the test compound was added and subjected to twofold serial dilutions, resulting in final concentrations between 1000 µg/mL and 1.95 µg/mL. For controls, row 11 contained 30 µL of broth and 30 µL of tetracycline (1000 µg/mL) as the positive control, while row 12 contained 30 µL of broth and 30 µL of 10% DMSO as the negative control. Each well was then filled with 10 µL of bacterial suspension (1×10^8 CFU/mL) and 30 µL of 0.02% resazurin. The plates were incubated at 37 °C for 6 h. The MIC was defined as the lowest concentration at which no visible color change occurred, indicating bacterial growth inhibition.

4.12. Fungal Cultures

The plant pathogenic fungi *M. fructigena* and *V. dahliae* were obtained from stock cultures at the Phytopathology Laboratories, Department of Plant Protection, Faculty of Agriculture, Kırşehir Ahi Evran University. Cultures were incubated at 23 ± 2 °C for 7 days in 90 mm Petri dishes containing 20 mL of potato dextrose agar (PDA), a nutrient-rich medium supporting fungal growth and morphological characterization. PDA was selected to maintain optimal fungal development and preserve the pathogens' physiological characteristics and infective capacity under standard conditions.

4.13. Antifungal Activity

The antifungal activity of the plant extract and AgNPs was determined using a modified agar plate method.[101,102] A stock solution was prepared by dissolving the methanol extract obtained from TP and AgNPs in 1% DMSO. PDA was autoclaved, cooled to 40 °C, and mixed with the plant extract at concentrations of 0 (control), 50, 100, 200, and 400 ppm. A volume of 10 mL of PDA was poured into 60-mm Petri dishes. Mycelial disks (5 mm) from 7-day-old fungal cultures were placed at the center of each dish. Following inoculation, cultures were incubated at 23 ± 2 °C for 10 days, and fungal growth was monitored daily. Colony diameters were measured in two perpendicular directions. Mycelial growth inhibition (%) was calculated using the following formula.[103]

$$I = 100 \times (d_c - d_t)/dc$$

where I is the inhibition percentage, d_c is the colony diameter in the control, and d_t is the diameter in the treatment group. A 5% (v/v) DMSO solution was used as a negative control. As a positive control, the standard fungicide Thiram 80% was used. All tests were performed in triplicate and repeated twice.

4.14. Statistical Analysis

Data are presented as means ± SEM from experiments performed in triplicate. Statistical evaluation was conducted using SPSS version 15.0. One-way ANOVA was performed to assess differences among groups, followed by Duncan and Tukey post-hoc tests, with $p < 0.05$ considered statistically significant.

© 2025 Wiley-VCH GmbH

23656549, 2025, 38, Downloaded from https://chemistry-europe.onlinelibrary.wiley.com/doi/10.1002/slct.202503764 by Samed MEK - Erzincan Universitesi , Wiley Online Library on [11/10/2025]. See the Terms and Conditions (https://onlinelibrary.wiley.com/terms-and-conditions) on Wiley Online Library for rules of use; OA articles are governed by the applicable Creative Commons License

Acknowledgments

The author sincerely thank Prof. Dr. Ali Kandemir for his invaluable contributions to the collection and taxonomic identification of the plant sample used in this study. This research received no external funding.

Conflict of Interests

The author declares no conflict of interest.

Keywords: Biological activity · Green synthesis · Nanobiotechnology · Silver nanoparticles · *Thymus pectinatus*

[1] T. Ç. Akman, S. Şimşek, Z. Akşit, H. Akşit, A. Aydin, A. R. Tüfekçi, S. Adem, M. A. Yilmaz, *J. Sci. Food Agric.* **2024**, *104*, 4039–4049, https://doi.org/10.1002/jsfa.13286.
[2] R. Shrivastava, J. Mishra, *J. Drug. Deliv. Ther.* **2019**, *9*, 107–113, https://doi.org/10.22270/jddt.v9i3.2608.
[3] K. S. Abdel Lateif, I. A. Maghrabi, H. A. Eldeab, *J. Bioprocess. Biotechnol.* **2016**, *6*, 293, https://doi.org/10.4172/2155-9821.1000293.
[4] E. K. Davison, M. A. Brimble, *Curr. Opin. Chem. Biol.* **2019**, *52*, 1–8, https://doi.org/10.1016/j.cbpa.2018.12.007.
[5] M. C. Bergonzi, C. M. Heard, J. Garcia-Pardo, *Pharmaceutics* **2022**, *14*, 2116, https://doi.org/10.3390/pharmaceutics14102116.
[6] R. C. C. da Silva, M. C. S. Alves, D. F. Matos, S. A. C. Quaresma, *Concilium* **2024**, *24*, 104.
[7] J. W.-H. Li, J. C. Vederas, *Science* **2009**, *325*, 161–165, https://doi.org/10.1126/science.1168243.
[8] H. Aksit, Y. Bayar, S. Simsek, Y. Ulutas, *J. Essent. Oil-Bear. Plants* **2022**, *25*, 200–207, https://doi.org/10.1080/0972060X.2022.2043189.
[9] R. R. Raja, *Res. J. Med. Plant* **2012**, *6*, 203.
[10] F. Anwar, R. K. Mahrye, R. Qadir, S. Saadi, E. Gruczynska-Sekowska, N. Saari, F. Hossain Brishti, *Chem. Biodivers.* **2024**, *21*, e202400500.
[11] X. Li, T. He, X. Wang, M. Shen, X. Yan, S. Fan, L. Wang, X. Wang, X. Xu, H. Sui, G. She, *Chem. Biodivers.* **2019**, *16*, e1900254, https://doi.org/10.1002/cbdv.201900254.
[12] A. S. Oliveira, C. Cavaleiro, J. Martinez-de-Oliveira, A. Palmeira-de-Oliveira, *Rev. Bras. Farmacogn.* **2023**, *33*, 1089.
[13] S. M. Patil, R. Ramu, P. S. Shirahatti, C. Shivamallu, R. G. Amachawadi, *Heliyon* **2021**, *7*, e07054.
[14] A. Chaudhary, D. Singh, *Gene Rep.* **2022**, *27*, 101533, https://doi.org/10.1016/j.genrep.2022.101533.
[15] J. Hrustić, M. Mihajlović, M. Grahovac, G. Delibašić, A. Bulajić, B. Krstić, B. Tanović, *Pestic. Fitomed.* **2012**, *27*, 283.
[16] D. Abate, C. Pastore, D. Gerin, R. De Miccolis Angelini, C. Rotolo, S. Pollastro, F. Faretra, *Plant Dis* **2018**, *102*, 1708–1717, https://doi.org/10.1094/PDIS-08-17-1314-RE.
[17] W. Zhou, X. Zhang, *Mol. Plant* **2021**, *14*, 1785.
[18] A. K. Wallace, *Trends Biotechnol.* **2023**, *41*, 1096–1097, https://doi.org/10.1016/j.tibtech.2023.03.017.
[19] D. A. Lomelí-Rosales, A. Zamudio-Ojeda, O. K. Reyes-Maldonado, M. E. López-Reyes, G. C. Basulto-Padilla, E. J. Lopez-Naranjo, V. M. Zuñiga-Mayo, G. Velázquez-Juárez, *Molecules* **2022**, *27*, 1692, https://doi.org/10.3390/molecules27051692.
[20] A. Shahverdi, A. Fakhimi, G. Mosavat, P. Jafari-Fesharaki, S. Rezaie, S. Rezayat, *World Appl. Sci. J.* **2010**, *10*, 918.
[21] M. S. AlSalhi, K. Elangovan, A. J. A. Ranjitsingh, P. Murali, S. Devanesan, *Saudi J. Biol. Sci.* **2019**, *26*, 970–978, https://doi.org/10.1016/j.sjbs.2019.04.001.
[22] Z. Villagrán, L. M. Anaya-Esparza, C. A. Velázquez-Carriles, J. M. Silva-Jara, J. M. Ruvalcaba-Gómez, E. F. Aurora-Vigo, E. Rodríguez-Lafitte, N. Rodríguez-Barajas, I. Balderas-León, F. Martínez-Esquivias, *Resources* **2024**, *13*, 70, https://doi.org/10.3390/resources13060070.
[23] Y. Bao, J. He, K. Song, J. Guo, X. Zhou, S. Liu, *J. Chem.* **2021**, *2021*, 1–14, https://doi.org/10.1155/2021/6562687.
[24] O. Velgosova, L. Veselovský, *Mater. Lett.* **2019**, *248*, 150–152, https://doi.org/10.1016/j.matlet.2019.04.027.
[25] M. Muntasir Alam Muhib, M. Mubassira, S. Khanam, S. Abeed-Ul-Haque, M. Faruk Hasan, *World J. Adv. Res. Rev. Food Agric.* **2024**, *21*, 1221–1238, https://doi.org/10.30574/wjarr.2024.21.3.0744.
[26] V. Sharma, R. Yngard, Y. Lin, *Adv. Colloid Interface Sci.* **2009**, *145*, 83–96, https://doi.org/10.1016/j.cis.2008.09.002.
[27] M. S. Panwar, P. Pal, D. Joshi, *J. Drug Deliv. Ther.* **2024**, *14*, 177–184, https://doi.org/10.22270/jddt.v14i11.6854.
[28] W. A. Shaikh, S. Chakraborty, G. Owens, R. U. Islam, *Appl. Nanosci.* **2021**, *11*, 2625–2660, https://doi.org/10.1007/s13204-021-02135-5.
[29] H. Singh, M. F. Desimone, S. Pandya, S. Jasani, N. George, M. Adnan, A. Aldarhami, A. S. Bazaid, S. A. Alderhami, *Int. J. Nanomed.* **2023**, *18*, 4727.
[30] T. Ghosh, A. Chattopadhyay, A. C. Mandal, S. Pramanik, P. K. Kuiri, *Chin. J. Phys.* **2020**, *68*, 835–848, https://doi.org/10.1016/j.cjph.2020.10.025.
[31] G. Hashemitabar, F. Aflakian, A. H. Sabzevar, *J. Mol. Struct.* **2023**, *1291*, 136076, https://doi.org/10.1016/j.molstruc.2023.136076.
[32] S. B. Parit, V. C. Karade, R. B. Patil, N. V. Pawar, R. P. Dhavale, M. Tawre, K. Pardesi, U. U. Jadhav, V. V. Dawkar, R. S. Tanpure, J. H. Kim, J. P. Jadhav, A. D. Chougale, *Mater. Today Chem.* **2020**, *17*, 100285, https://doi.org/10.1016/j.mtchem.2020.100285.
[33] J. Lee, H. Y. Kim, H. Zhou, S. Hwang, K. Koh, D.-W. Han, J. Lee, *J. Mater. Chem.* **2011**, *21*, 13316, https://doi.org/10.1039/c1jm11592h.
[34] J. Singh, T. Dutta, K.-H. Kim, M. Rawat, P. Samddar, P. Kumar, *J. Nanobiotechnol.* **2018**, *16*, 1–24, https://doi.org/10.1186/s12951-018-0408-4.
[35] A. Elbourne, R. J. Crawford, E. P. Ivanova, *J. Colloid Interface Sci.* **2017**, *508*, 603–616, https://doi.org/10.1016/j.jcis.2017.07.021.
[36] S. Pal, Y. K. Tak, J. M. Song, *Appl. Environ. Microbiol.* **2007**, *73*, 1712–1720, https://doi.org/10.1128/AEM.02218-06.
[37] J. Ren, W. Wang, S. Sun, L. Zhang, L. Wang, J. Chang, *Ind. Eng. Chem. Res.* **2011**, *50*, 10366.
[38] S. Kummara, M. B. Patil, T. Uriah, *Biomed. Pharmacother.* **2016**, *84*, 10–21, https://doi.org/10.1016/j.biopha.2016.09.003.
[39] K. Rani, *IP Int. J. Compr. Adv. Pharmacol.* **2020**, *5*, 9–13, https://doi.org/10.18231/j.ijcaap.2020.003.
[40] A. S. Barnard, *Acc. Chem. Res.* **2012**, *45*, 1688–1697, https://doi.org/10.1021/ar3000184.
[41] A. M. Steiner, M. Mayer, D. Schletz, D. Wolf, P. Formanek, R. Hübner, M. Dulle, S. Förster, T. A. F. König, A. Fery, *Chem. Mater.* **2019**, *31*, 2822–2827, https://doi.org/10.1021/acs.chemmater.8b05220.
[42] J. Chaudhary, G. Tailor, M. Yadav, C. Mehta, *Biocatal. Agric. Biotechnol.* **2023**, *50*, 102692, https://doi.org/10.1016/j.bcab.2023.102692.
[43] G. Marslin, K. Siram, Q. Maqbool, R. K. Selvakesavan, D. Kruszka, P. Kachlicki, G. Franklin, *Mater. Res. Express* **2018**, *11*, 940.
[44] B. Nickavar, N. J. Esbati, *J. Acupunct. Meridian Stud.* **2012**, *5*, 119.
[45] E. Eroglu Ozkan, E. Ersoy, Y. Yesil Canturk, E. Mataraci Kara, E. Cinar, H. Sahin, S. Karahan, K. Karaca Sancaktepe, M. A. Yilmaz, M. Boga, *Front. Pharmacol.* **2022**, *13*, 923063, https://doi.org/10.3389/fphar.2022.923063.
[46] C. Ballester-Costa, E. Sendra, J. Fernández-López, J. A. Pérez-Álvarez, M. J. Viuda-Martos, *Foods* **2017**, *6*, 59, https://doi.org/10.3390/foods6080059.
[47] B. Tepe, M. Sokmen, H. A. Akpulat, D. Daferera, M. Polissiou, A. Sokmen, *J. Food Eng.* **2005**, *66*, 447–454, https://doi.org/10.1016/j.jfoodeng.2004.04.015.
[48] A. F. Afonso, O. R. Pereira, S. M. Cardoso, *Antioxidants* **2020**, *9*, 814, https://doi.org/10.3390/antiox9090814.
[49] M. Wahab, A. Bhatti, P. John, *Polymers* **2022**, *14*, 3138, https://doi.org/10.3390/polym14153138.
[50] S. Aldosary, S. El-Rahman, S. Al-Jameel, N. Alromihi, *Braz. J. Biol.* **2021**, *83*, e244675.
[51] U. Ejaz, M. Afzal, M. Mazhar, M. Riaz, N. Ahmed, W. Y. Rizg, A. A. Alahmadi, M. Y. Badr, R. Y. Mushtaq, C. Y. Yean, *Int. J. Nanomed.* **2024**, *19*, 453–469, https://doi.org/10.2147/IJN.S446017.
[52] S. M. Alnasser, *Pol. J. Environ. Stud.* **2023**, *32*, 5469.
[53] S. Palmieri, M. Pellegrini, A. Ricci, D. Compagnone, C. Lo Sterzo, *Foods* **2020**, *9*, 1221, https://doi.org/10.3390/foods9091221.
[54] M. Babotă, O. Frumuzachi, A. Gâvan, C. Iacoviță, J. Pinela, L. Barros, I. C. F. R. Ferreira, L. Zhang, L. Lucini, G. Rocchetti, C. Tanase, G. Crișan, A. Mocan, *Ultrason. Sonochem.* **2022**, *84*, 105954, https://doi.org/10.1016/j.ultsonch.2022.105954.

© 2025 Wiley-VCH GmbH

[55] A. R. S. Mateus, C. Serrano, C. Almeida, A. Soares, V. R. Lopes, A. Sanches-Silva, *Appl. Sci.* **2024**, *14*, 8924.
[56] A. Gedikoğlu, M. Sökmen, A. Çivit, *Food Sci. Nutr.* **2019**, *7*, 1704–1714, https://doi.org/10.1002/fsn3.1007.
[57] W. Megdiche-Ksouri, M. Saada, B. Soumaya, M. Snoussi, Y. Zaouali, R. Ksouri, *New Sci.* **2015**, *23*, 1046.
[58] A. Afreen, R. Ahmed, S. Mehboob, M. Tariq, H. A. Alghamdi, A. A. Zahid, I. Ali, K. Malik, A. Hasan, *Mater. Res. Express* **2020**, *7*, 075404.
[59] S. S. Zahra, M. Ahmed, M. Qasim, B. Gul, M. Zia, B. Mirza, I.-u. Haq, *BMC Complement. Altern. Med.* **2017**, *17*, 443, https://doi.org/10.1186/s12906-017-1951-5.
[60] T. Narangerel, M. Sójka, R. Bonikowski, K. Jastrząbek, W. Sroczyński, A. Plucińska, A. Kunicka-Styczyńska, K. Śmigielski, I. Majak, A. Bartos, J. Leszczyńska, *Antioxidants* **2021**, *10*, 1905, https://doi.org/10.3390/antiox10121905.
[61] B. Shahar, A. Indira, O. Santosh, N. Dolma, N. Chongtham, *Measure. Food* **2023**, *10*, 100092.
[62] R. Jaouadi, A. M. Silva, M. Boussaid, I. B. Yahia, S. M. Cardoso, Y. Zaouali, *Antioxidants* **2019**, *8*, 515, https://doi.org/10.3390/antiox8110515.
[63] M. J. Jordán, R. M. Martínez, C. Martínez, I. Moñino, J. A. Sotomayor, *Ind. Crops Prod.* **2009**, *29*, 145–153, https://doi.org/10.1016/j.indcrop.2008.04.021.
[64] A. F. Afonso, O. R. Pereira, M. Válega, A. M. Silva, S. M. Cardoso, *Molecules* **2018**, *23*, 1514, https://doi.org/10.3390/molecules23071514.
[65] H. Jangid, H. C. Joshi, J. Dutta, A. Ahmad, M. B. Alshammari, K. Hossain, G. Pant, G. Kumar, *Food Chem. X* **2025**, *26*, 102298.
[66] A. Miskovska, M. Kulisova, O. Matatkova, J. Michailidu, A. Cejkova, I. J. Kolouchova, *Environ. Technol. Innov.* **2025**, *39*, 104287, https://doi.org/10.1016/j.eti.2025.104287.
[67] G. Vardar-Ünlü, F. Candan, A. Sökmen, D. Daferera, M. Polissiou, M. Sökmen, E. Dönmez, B. Tepe, *J. Agric. Food Chem.* **2003**, *51*, 63–67, https://doi.org/10.1021/jf025753e.
[68] M. Ghavam, G. Bacchetta, I. Castangia, M. L. Manca, *Sci. Rep.* **2022**, *12*, 17044.
[69] A. Jayari, A. Jouini, H. Boukhris, S. Hamrouni, C. Damergi, S. Ben Hadj Ahmed, A. Maaroufi, *J. Food Qual.* **2021**, *2021*, 5599374.
[70] M. Kačániová, S. Garzoli, A. Ben Hsouna, A. Bianchi, M. I. Kluz, J. H. Elizondo-Luevano, Z. Ban, R. Ben Saad, W. Mnif, P. Haščík, *Foods* **2024**, *13*, 3107.
[71] S. Jilani, M. Ferjeni, K. Al-Shammery, H. Rashid Mohammed AlTamimi, M. Besbes, S. Ahmed Lotfi, A. Farouk, W. Ben Selma, *Front. Pharmacol.* **2025**, *16*, 1582102, https://doi.org/10.3389/fphar.2025.1582102.
[72] Z. Maksimović, M. Milenković, D. Vučićević, M. Ristić, *Cent. Eur. J. Biol.* **2008**, *3*, 149.
[73] M. Gholami, K. Shahzamani, A. Marzban, H. E. Lashgarian, *IET Nanobiotechnol* **2018**, *12*, 1114–1117, https://doi.org/10.1049/iet-nbt.2018.5110.
[74] F. Erci, E. Torlak, *Sak. Univ. J. Sci.* **2019**, *23*, 333.
[75] A. Balciunaitiene, P. Viskelis, J. Viskelis, P. Streimikyte, M. Liaudanskas, E. Bartkiene, P. Zavistanaviciute, E. Zokaityte, V. Starkute, M. Ruzauskas, V. Lele, *Processes* **2021**, *9*, 1304, https://doi.org/10.3390/pr9081304.
[76] D. A. Abdel-Moneam, H. S. Khalefa, M. M. Rashad, G. E. Ali, Y. H. Ahmed, E. Ragab, O. A. Fouad, R. A. Geioushy, S. B. Mahmoud, *Fish Physiol. Biochem.* **2025**, *51*, 146, https://doi.org/10.1007/s10695-025-01560-5.
[77] M. Moazeni, A. Davari, S. Shabanzadeh, J. Akhtari, M. Saeedi, K. Mortyeza-Semnani, M. Abastabar, M. Nabili, F. H. Moghadam, B. Roohi, *J. Herb. Med.* **2021**, *28*, 100452.
[78] M. N. Boukhatem, N. H. Darwish, T. Sudha, S. Bahlouli, D. Kellou, A. B. Benelmouffok, H. Chader, M. Rajabi, Y. Benali, S. A. Mousa, *Sci. Pharm.* **2020**, *88*, 33.
[79] Z. Hadi, A. Ferdousi, M. Paknejadi, *Arch. Razi Inst.* **2024**, *79*, 973.
[80] M. Roxo, M. Zuzarte, M. J. Gonçalves, J. M. Alves-Silva, C. Cavaleiro, M. T. Cruz, L. Salgueiro, *Sci. Rep.* **2020**, *10*, 18859, https://doi.org/10.1038/s41598-020-75244-w.
[81] S. Boukhira, F. E.-Z. Amrati, M. Chebaibi, A. Grafov, R. A. Mothana, H. M. Al-Yousef, D. Bousta, *Front. Chem.* **2024**, *12*, 1402310, https://doi.org/10.3389/fchem.2024.1402310.
[82] M. Moshaverinia, S. Sahmeddini, F. Lavaee, Z. Zareshahrabadi, K. Zomorodian, *Biomed. Res. Int.* **2022**, *2022*, 9744153.
[83] R. Farrukh, M. Zargar, A. Akhtar, S. Tasduq, S. Surjeet, U. Nissar, S. Rakhshanda, A. Masood, S. Ganie, A. Shajrul, *Bot. Res. Int.* **2012**, *5*, 36.
[84] A. S. Doghish, A. M. Shehabeldine, H. A. El-Mahdy, M. M. Hassanin, A. A. Al-Askar, S. A. Marey, H. AbdElgawad, A. H. Hashem, *Molecules* **2023**, *28*, 6910, https://doi.org/10.3390/molecules28196910.
[85] A. Vitali, A. Stringaro, M. Colone, A. Muntiu, L. Angiolella, *Antibiotics* **2021**, *11*, 11, https://doi.org/10.3390/antibiotics11010011.
[86] K. Pietrzak, S. Glińska, M. Gapińska, T. Ruman, A. Nowak, E. Aydin, B. Gutarowska, *Metallomics* **2016**, *8*, 1294–1302, https://doi.org/10.1039/C6MT00161K.
[87] S. Saqib, S. Faryad, M. I. Afridi, B. Arshad, M. Younas, M. Naeem, W. Zaman, F. Ullah, M. Nisar, S. Ali, A. M. Elgorban, A. Syed, H. O. Elansary, T. K. Z. El-Abedin, *Coatings* **2022**, *12*, 1505, https://doi.org/10.3390/coatings12101505.
[88] T. Ç. Akman, S. Şimşek, Z. Akşit, A. Aydın, M. A. Yılmaz, *KSÜ Tar. Doga Derg.* **2024**, *27*, 782.
[89] G. Adıgüzelli, E. Osma, T. Varol, S. Şimşek, A. Kandemir, *Osmaniye Korkut Ata Univ. J. Sci. Inst.* **2024**, *7*, 2315.
[90] T. Varol, E. Osma, S. Şimşek, M. Elveren, *Front. Life Sci.* **2023**, *4*, 150–156, https://doi.org/10.51753/flsrt.1357325.
[91] Z. Akşit, H. Akşit, S. Şimşek, A. Aydın, M. Yılmaz, A. Kandemir, E. Köksal, *Pharm. Pharmacol. Int. J.* **2022**, *10*, 190.
[92] S. Şimşek, *Erzincan Univ. J. Sci. Technol.* **2025**, *18*, 391.
[93] S. Şimşek, H. Akşit, A. Aydın, E. Köksal, *Chem. Biodivers.* **2023**, *20*, e202301200.
[94] E. N. Albayrak, S. Şimşek, A. B. Musatat, Z. Akşit, H. Akşit, A. Atahan, *J. Sci. Technol.* **2024**, *12*, 981.
[95] S. Şimşek, T. Varol, Z. Akşit, M. Elveren, E. Osma, *N. Z. J. Bot.* **2025**, *63*, 1.
[96] F. R. Alkan, B. Çetiner, H. Akşit, S. Şimşek, *Turk. J. Agric. Food Sci. Technol.* **2025**, *13*, 1937.
[97] S. Gözcü, Z. Akşit, S. Şimşek, A. Kandemir, A. Aydın, M. A. Yılmaz, H. Akşit, *J. Res. Pharm.* **2024**, *28*, 961.
[98] S. Gözcü, Z. Akşit, S. Şimşek, A. Kandemir, A. Aydın, M. A. Yılmaz, H. Akşit, *J. Sci. Food Agric.* **2024**, *104*, 1382.
[99] S. Gözcü, Z. Akşit, S. Şimşek, H. Akşit, *Chem. Biodivers.* **2025**, e00455.
[100] S. Gözcü, Z. Akşit, A. Aydın, M. A. Yılmaz, S. Şimşek, *Nat. Prod. Res.* **2025**, *39*, 633–644.
[101] Z. Akşit, M. Ç. Fırat, H. Akşit, Y. Bayar, M. Alkan, S. Şimşek, *J. Essent. Oil Bear. Plants* **2024**, *27*, 374.
[102] H. Akşit, S. Şimşek, A. Aydın, Y. Bayar, M. J. F. Alkan, *Flavour Fragr. J.* **2025**, *40*, 665.
[103] S. Şimşek, H. Akşit, Y. Bayar, T. Karakurt, *ChemistrySelect* **2025**, *10*, e202400701.

Manuscript received: June 28, 2025

© 2025 Wiley-VCH GmbH

23656549, 2025, 38, Downloaded from https://chemistry-europe.onlinelibrary.wiley.com/doi/10.1002/slct.202503764 by Samed MEK - Erzincan Universitesi , Wiley Online Library on [11/10/2025]. See the Terms and Conditions (https://onlinelibrary.wiley.com/terms-and-conditions) on Wiley Online Library for rules of use; OA articles are governed by the applicable Creative Commons License